

adsorb in a regular array and which will show atomic diffraction that can potentially be analyzed for definitive structure determination. This should be applicable for insulator and semiconductor surfaces in addition to metal surfaces, and the difficulty of surface charging which is present with electron diffraction is obviated with diffraction of neutrals. As an example, when H_2 adsorbs atomically in a (1×1) array on the tungsten carbide surface, the zero-, first-, and second-order diffraction peaks, though somewhat attenuated, can still be resolved. Such experiments designed to explore the range of adsorbates which exhibit He diffraction are continuing in this laboratory.

A more complete presentation of the diffraction of He and D_2 from the $R(3 \times 5)$ tungsten carbide, as well as Ne and Ar scattering from that surface, and He and D_2 scattering from a (1×1) tungsten carbide surface will be presented in a future publication.

One of us (W.H.W.) acknowledges the support of a National Defense Education Act pre-doctoral fellowship.

*Work supported by U. S. Air Force Office of Scientific Research Grant No. 68-1409.

¹C. J. Davisson and L. H. Germer, Phys. Rev. **30**, 705 (1927).

²I. Estermann and O. Stern, Z. Phys. **61**, 95 (1930).

³I. Estermann, R. Frisch, and O. Stern, Z. Phys. **73**, 348 (1931).

⁴R. Frisch and O. Stern, Z. Phys. **84**, 430 (1933).

⁵R. Frisch, Z. Phys. **84**, 443 (1933).

⁶T. H. Johnson, Phys. Rev. **37**, 847 (1931).

⁷J. C. Crews, J. Chem. Phys. **37**, 2004 (1962).

⁸J. C. Crews, in *Fundamentals of Gas Surface Interactions*, edited by H. Saltsburg, J. N. Smith, Jr., and M. Rogers (Academic, New York, 1967), p. 480.

⁹S. S. Fisher, M. N. Bishara, A. R. Kuhlthau, and J. E. Scott, Jr., in *Proceedings of the Sixth International Symposium on Rarefied Gas Dynamics, Massachusetts Institute of Technology, Cambridge, Mass., 1968*, edited by L. Trilling and H. Y. Wachman (Academic, New York, 1969), Vol. II, p. 1227.

¹⁰J. R. Bledsoe, S. S. Fisher, and J. E. Scott, Jr., Bull. Amer. Phys. Soc. **13**, 1601 (1968).

¹¹D. R. O'Keefe, R. L. Palmer, H. Saltsburg, and J. N. Smith, Jr., J. Chem. Phys. **49**, 5194 (1968).

¹²D. R. O'Keefe, J. N. Smith, Jr., R. L. Palmer, and H. Saltsburg, Surface Sci. **20**, 27 (1970).

¹³D. R. O'Keefe, J. N. Smith, Jr., R. L. Palmer, and H. Saltsburg, J. Chem. Phys. **52**, 4447 (1970).

¹⁴R. L. Palmer, H. Saltsburg, and J. N. Smith, Jr., J. Chem. Phys. **50**, 4661 (1969).

¹⁵A. G. Stoll, Jr., and R. P. Merrill, to be published.

¹⁶R. M. Stern, Appl. Phys. Lett. **5**, 218 (1964).

¹⁷D. L. Smith and R. P. Merrill, J. Chem. Phys. **52**, 5861 (1970).

¹⁸To calculate the wavelength the average kinetic energy of the incident beam is added to an estimate of the potential well for the He-WC surface to determine the momentum: $p^2/2m = 2kT + D$; for $D = 200$ cal/mole, $\lambda = h/p = 0.588 \text{ \AA}$ at 295°K. If $D = 0$ then $\lambda = 0.635 \text{ \AA}$ at 295°K.

¹⁹The specular maximum of D_2 at $\theta_i = 45^\circ$, $T_s = 625^\circ\text{K}$ is about 5%, while the specular maximum of He under the same conditions is about 50% of the incident-beam intensity for this tungsten carbide surface.

²⁰W. H. Weinberg and R. P. Merrill, to be published.

²¹D. L. Smith and R. P. Merrill, to be published.

Experimental Verification of First-Order Rotational Effects in the Magnetoelastic Properties of an Antiferromagnet*

R. L. Melcher

IBM Watson Research Center, Yorktown Heights, New York 10598

(Received 27 August 1970)

The experimental magnetoelastic properties of antiferromagnetic MnF_2 are found in certain specific instances to be completely inconsistent with the usual small-strain magnetoelastic theory. Rigorous application of finite-deformation magnetoelastic theory including the effect of the rotational component of the shear deformation leads to results which are in excellent agreement with experiment.

The purpose of this paper is to provide experimental verification of finite-deformation magnetoelastic theory when applied to an antiferromagnetic, elastic medium. It will be shown that the neglect of the rotational component of an elastic shear deformation by the usual small-strain mag-

netoelastic theory^{1,2} leads to first-order results both qualitatively and quantitatively inconsistent with experiment. This is the first experimental demonstration of the validity of finite-deformation theory for an antiferromagnet. Eastman³ has shown that magnetoelastic effects in yttrium iron

garnet (YIG) are properly accounted for only through the use of finite-deformation theory. In the present case of the nominally uniaxial antiferromagnet MnF_2 , the significant difference between the small-strain and the finite-deformation theories arises from terms in the local internal energy properly ignored by Eastman in his treatment of YIG but dominant in the magnetoelastic behavior of MnF_2 . Finally, it is suggested that finite-deformation theory provides an explanation for the anomalous behavior reported by Shapira and Zak for the attenuation of the elastic mode corresponding to the elastic constant c_{44} near the spin-flop transition in MnF_2 .⁴

The conventional small-strain theory^{1,2} as-

$$U = -\lambda\rho\vec{m}_1 \cdot \vec{m}_2 - \frac{1}{2}\frac{K}{\rho m_s}(m_{1x}^2 + m_{2x}^2) + \frac{b}{\rho m_s}[(m_{1x}-m_{2x})e_{xz} + (m_{1y}-m_{2y})e_{yz}] + \frac{1}{2\rho}c_{44}(e_{xz}^2 + e_{yz}^2), \quad (2)$$

where ρ is the mass density and $m_s^2 = \vec{m}_1 \cdot \vec{m}_1 = \vec{m}_2 \cdot \vec{m}_2$. Only those terms of the elastic energy relevant to the present discussion have been included and the magnetoelastic coupling term is correct to first order in the strain e_{ij} . Equations of motion for the elastic and magnetic variables can be derived from this form of the local internal energy. Assuming the dc magnetic field to be applied along the "easy" or [001] axis and solving the coupled equations of motion for the effective shear elastic constant c_{44}^* , the following expression is obtained

$$c_{44}^* = c_{44} - \frac{2b^2}{K} \left(\frac{H_c^2}{H_c^2 - H_0^2} \right). \quad (3)$$

The spin-flop field H_c is given by $(2H_E H_A)^{1/2}$ where $H_E = -\lambda\rho m_s$ and $H_A = K/\rho m_s$ and this result is valid only for $H_0 < H_c$ and $\omega \ll \gamma(H_c - H_0)$. Because of the symmetry of the stress tensor derived from Eq. (2) this solution holds for shear waves propagating along the [001] axis with arbitrary polarization or propagating perpendicular to the [001] axis and polarized along this axis.⁶

The above small-strain formulation of the problem has been criticized by several authors⁷⁻⁹ primarily on the basis that fundamental conservation laws are applied separately to the rigid magnetic system and the nonmagnetic elastic system. In particular, the internal energy U of Eqs. (1) and (2) is not in general rotationally invariant and therefore the system described by these equations does not conserve total angular momentum. The use of finite-deformation theory¹⁰ and consistent application of conservation laws to the total magnetomechanical system leads to a local in-

ternal energy which satisfies the necessary invariance conditions. In the long wavelength limit⁵ this general energy function for an antiferromagnet can be constructed with the variables¹¹

$$U = U_M(m_{ij}) + U_E(e_{ij}) + U_{ME}(m_{ij}, e_{kl}), \quad (1)$$

where U_M is the energy of the rigid magnetic system, U_E corresponds to the nonmagnetic elastic system, and U_{ME} is an interaction energy. Here m_{ij} is the j th ($j=x, y, z$) component of the i th ($i=1, 2$) sublattice magnetic moment per unit mass and e_{ij} are the symmetric infinitesimal strain components.⁵ Considering a uniaxial antiferromagnet described by an anisotropy constant K , exchange constant λ , magnetoelastic coupling constant b , and shear elastic constant c_{44} , the function U takes the form

ternal energy which satisfies the necessary invariance conditions. In the long wavelength limit⁵ this general energy function for an antiferromagnet can be constructed with the variables¹¹

$$m_{jk}^* \equiv m_{ji} \frac{\partial x_i}{\partial a_k}, \quad C_{kl} \equiv \frac{\partial x_i}{\partial a_k} \frac{\partial x_i}{\partial a_l}, \quad (4)$$

where $\partial x_i / \partial a_k$ is a component of the finite-deformation tensor; (x_1, x_2, x_3) is the instantaneous position of a material particle whose natural position is given by (a_1, a_2, a_3) and $q_i \equiv x_i - a_i$.⁷⁻¹⁰ Constructing the function U in this manner and expanding to second order in the small quantities m_{1x} , m_{2x} , m_{1y} , m_{2y} , and the displacement gradients $\partial q_i / \partial a_j = \partial x_i / \partial a_j - \delta_{ij}$ leads to the terms given in Eq. (2) plus the additional terms $U_{K'}$ and U_{ME}' :

$$U_{K'} = -\frac{1}{2} \frac{K}{\rho m_s} [(m_{1x}-m_{2x})\Omega_{xz} + (m_{1y}-m_{2y})\Omega_{yz}] - \frac{K}{\rho} e_{zz}^2, \quad (5)$$

$$U_{ME}' = b[e_{xz}^2 + e_{yz}^2 + e_{xz}\Omega_{xz} + e_{yz}\Omega_{yz}], \quad (6)$$

where $\Omega_{ij} \equiv \partial q_j / \partial a_i - \partial q_i / \partial a_j$ is twice the rotational part of the displacement gradient $\partial q_j / \partial a_i = \frac{1}{2}(e_{ij} + \Omega_{ij})$. The antisymmetrical parts of $U_{K'}$ and U_{ME}' clearly lead to antisymmetric terms in the stress tensor—terms not included in the small-strain approximation. Including the effects of $U_{K'}$ and U_{ME}' , the solutions to the equations of motion take the form

$$c_{44}^* = c_{44} - \frac{2(b - \frac{1}{2}K)^2}{K} \left(\frac{H_c^2}{H_c^2 - H_0^2} \right) \quad (7)$$

for shear waves propagating along the [001] axis and

$$c_{44}^* = c_{44} + 4b - \frac{2(b + \frac{1}{2}K)^2}{K} \left(\frac{H_c^2}{H_c^2 - H_0^2} \right) \quad (8)$$

for propagation perpendicular to the [001] axis and polarized along [001].¹² The difference between these two expressions is a consequence of the rotational part of the deformation gradient. The term on the right-hand side of Eq. (8), linear in b , derives from U_{ME}' and is similar in origin to the terms used by Eastman to show the validity of finite-deformation theory in YIG.³ The energy terms U_K' lead to the appearance of $b \pm \frac{1}{2}K$ in the magnetic-field-dependent part of Eqs. (7) and (8) rather than b as is found in the small-strain result Eq. (3). Terms similar to U_K' can be ignored in YIG since in that case $K \ll b$. On the other hand, in MnF_2 , K can be expected to be of the same order of magnitude as b ; therefore comparison of the field-dependent parts of Eq. (3) with those of Eqs. (7) and (8) is a sensitive and unambiguous test of the relative merit of the two theories.¹³

The results of measurements of the change in c_{44}^* as a function of the field dependent parameter $h \equiv H_0^2/(H_c^2 - H_0^2)$ for the propagation directions [001] and [110] in MnF_2 at 4.2°K are shown in Fig. 1. While the data for $\vec{k} \parallel [001]$ show the expected linear decrease with h (\vec{k} is the elastic wave vector), the data for $\vec{k} \parallel [110]$ are independent of h to a precision of $\pm 10^{-6}$. The results are in qualitative and quantitative disagreement with small-strain theory.

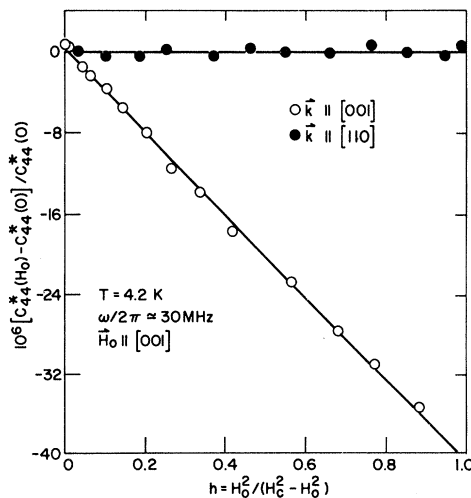


FIG. 1. The change in the effective elastic constant c_{44}^* for two propagation directions as a function of the magnetic-field dependent parameter $h \equiv H_0^2/(H_c^2 - H_0^2)$; $H_c = (2H_E H_A)^{1/2} \approx 93$ kOe.

The two sets of results for $\vec{k} \parallel [001]$ and $\vec{k} \perp [001]$ can be compared with finite-deformation theory as follows:

$$(b - \frac{1}{2}K)^2 / K = (6.5 \pm 1.3) \times 10^6 \text{ erg/cm}^3, \quad (9a)$$

$$(b + \frac{1}{2}K)^2 / K = (0 \pm 0.16) \times 10^6 \text{ erg/cm}^3, \quad (9b)$$

where the measured value $[0.32 \times 10^{12} \text{ dyne/cm}^2]$ of c_{44} has been used. Assuming that K lies within the accepted range of $(4.6-5.2) \times 10^6 \text{ erg/cm}^3$,^{14,15} agreement with both sets of data is found for $b = (-3.0 \pm 0.4) \times 10^6 \text{ erg/cm}^3$. Alternately, a value for b can be deduced independent of the value of K by subtracting Eq. (9b) from Eq. (9a). This results in $b = (-3.25 \pm 0.7) \times 10^6 \text{ erg/cm}^3$. With this value for b any value of K in the range $(4-10) \times 10^6 \text{ erg/cm}^3$ satisfies both Eqs. (9a) and (9b). These numerical results show that the experimental data are in excellent agreement with finite-deformation theory. Data taken with $\vec{k} \parallel [100]$ (not shown here) are identical to that for $\vec{k} \parallel [110]$; this is also in accord with the theory.

Figure 2 shows the behavior of c_{44}^* for the two propagation directions in the spin-flop region ($H_0 \approx H_c \approx 93$ kOe). The low-frequency approximation used in deriving Eqs. (7) and (8) is no longer valid and somewhat more general results have been obtained. These are, however, still characterized by the coupling constants $(b \pm \frac{1}{2}K)$. Again finite-deformation theory correctly predicts the experimentally observed asymmetry in the results for the two propagation directions. Inclusion of loss mechanisms results in the prediction of an ultrasonic absorption peak for ω

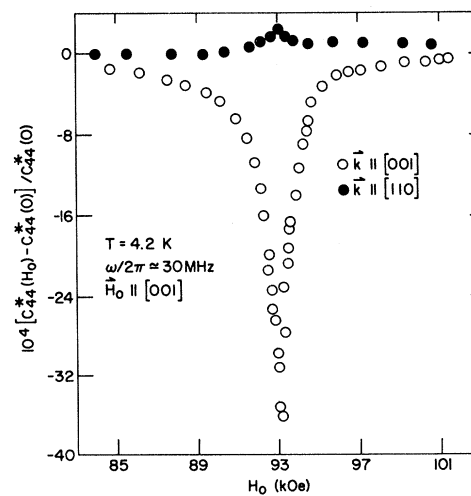


FIG. 2. The change in the effective elastic constant c_{44}^* for two propagation directions as a function of the magnetic field H_0 in the neighborhood of the spin-flop field $H_c \approx 93$ kOe.

$\approx \gamma(H_c - H_0)$ whose strength is characterized by $(b \pm \frac{1}{2}K)$. For $\omega < 10^9$ the resonance condition reduces effectively to $H_0 \approx H_c$. The ultrasonic attenuation corresponding to this elastic mode shows precisely the dependence on the propagation direction expected on the basis of the finite-deformation theory.⁴ The experimentally observed strong dependence of the attenuation on the orientation of the applied magnetic field is a consequence of the strong orientation dependence of the spin-wave frequencies themselves for $\omega/\gamma H_c \ll 1$.¹⁴

In conclusion, finite-deformation magnetoelastic theory is in excellent agreement with the experimental results presented here and also provides an alternate explanation independent of the existence of domains for the data of Shapira and Zak⁴ near the spin-flop transition. The usual small-strain theory, on the other hand, does not even provide a correct qualitative description of either set of data. This provides conclusive evidence that the rotational component of a shear deformation cannot in general be neglected even to first order when considering elastic phenomena in gyroscopic media. In particular, whenever the appropriate anisotropy and magnetoelastic coupling constants are comparable in magnitude, significant first-order rotational effects can be expected.¹⁵

The author is indebted to G. Burns, D. E. Eastman, E. Pytte, and A. W. Smith for criticisms of the manuscript.

*The experimental part of this paper was performed while the author was at Cornell University and was supported by the Advanced Research Projects Agency through the Materials Science Center at Cornell.

¹C. Kittel, Phys. Rev. **110**, 836 (1958).

²A. I. Akhiezer, V. G. Bar'yakhtar, and S. V. Peletminskii, Zh. Eksp. Teor. Fiz. **35**, 228 (1958) [Sov. Phys. JETP **8**, 157 (1959)].

³D. E. Eastman, Phys. Rev. **148**, 530 (1966).

⁴Y. Shapira and J. Zak, Phys. Rev. **170**, 503 (1968).

⁵For simplicity we restrict the discussion to an antiferromagnet in the long-wavelength approximation. Therefore, gradients of the sublattice magnetization need not be considered.

⁶A result similar to Eq. (3) was first obtained by S. V. Peletminskii, Zh. Eksp. Teor. Fiz. **452** (1959) [Sov. Phys. JETP **10**, 321 (1960)].

⁷K. B. Vlasov and B. Kh. Ishmukhametov, Zh. Eksp. Teor. Fiz. **46**, 201 (1964) [Sov. Phys. JETP **19**, 142 (1964)].

⁸H. F. Tierston, J. Math. Phys. **5**, 1298 (1964).

⁹W. F. Brown, Jr., J. Appl. Phys. **36**, 994 (1965).

¹⁰R. N. Thurston, in *Physical Acoustics*, edited by W. P. Mason (Academic, New York, 1964), Vol. IA.

¹¹V. G. Bar'yakhtar and V. V. Gann, Fiz. Tverd. Tela **9**, 2052 (1967) [Sov. Phys. Solid State **9**, 1611 (1968)].

¹²Expressions essentially equivalent to Eqs. (7) and (8) were first derived by V. V. Gann, Fiz. Tverd. Tela **9**, 3467 (1967) [Sov. Phys. Solid State **9**, 2734 (1968)].

¹³In a previous study of the low-field magnetoelastic properties of the MnF_2 [R. L. Melcher, J. Appl. Phys. **41**, 1412 (1970)] only $\hat{k} \parallel \hat{z}$ was studied experimentally, yielding fortuitous agreement with the small-strain theory.

¹⁴S. Foner, in *Magnetism*, edited by G. T. Rado and H. Suhl (Academic, New York, 1963), Vol. I.

¹⁵J. S. Smart, in *Magnetism*, edited by G. T. Rado and H. Suhl (Academic, New York, 1963), Vol. III.

¹⁶When $H_0 > H_c$ in MnF_2 , additional anisotropy (K') and magnetoelastic (b') constants become important. Since $b' \gg K'$ the two theories are essentially identical in the present approximation and in agreement with experiment [R. L. Melcher, Phys. Rev. Lett. **25**, 235 (1970)].

Effect of Spin-Lattice Coupling on the Critical Resistivity of a Ferromagnet*

F. C. Zumsteg, F. J. Cadieu, S. Marčelja,† and R. D. Parks

Department of Physics and Astronomy, University of Rochester, Rochester, New York 14627

(Received 17 July 1970)

Evidence is presented which demonstrates that the larger part of the anomaly above T_c in the c -axis electrical resistivity of gadolinium arises not from spin-disorder scattering but rather from the anomalous lattice contraction near T_c . The portion of the resistance anomaly attributable to spin-disorder scattering is monotonic in temperature and of the general form specified by the Fisher-Langer model.

Two general types of behavior have been observed for the temperature dependence of the electrical resistivity ρ of metallic ferromagnets: (1) a monotonic temperature dependence of ρ in the vicinity of T_c with a singularity in $d\rho/dT$ at

T_c , or (2) a nonmonotonic temperature dependence of ρ with a maximum in the vicinity of T_c . Examples of behavior (1) are found in nickel,^{1,2} iron,³ gadolinium (a axis),⁴ and various intermetallic compounds (e.g., $CdCo_2$)⁵; and examples of